NJC

Accepted Manuscript

This is an *Accepted Manuscript*, which has been through the Royal Society of Chemistry peer review process and has been accepted for publication.

Accepted Manuscripts are published online shortly after acceptance, before technical editing, formatting and proof reading. Using this free service, authors can make their results available to the community, in citable form, before we publish the edited article. We will replace this *Accepted Manuscript* with the edited and formatted *Advance Article* as soon as it is available.

You can find more information about *Accepted Manuscripts* in the Information for Authors.

Please note that technical editing may introduce minor changes to the text and/or graphics, which may alter content. The journal's standard Terms & Conditions and the Ethical guidelines still apply. In no event shall the Royal Society of Chemistry be held responsible for any errors or omissions in this *Accepted Manuscript* or any consequences arising from the use of any information it contains.

ROYAL SOCIETY OF CHEMISTRY

www.rsc.org/njc

New Journal of Chemistry

COMMUNICATION

A convenient 'NOSE' approach for the synthesis of 6-Amino-1,3-dimethyl-5-indolyl-1*H*-pyrimidine-2,4-dione derivatives catalyzed by nano-Ag

Received 00th January 20xx,
Accepted 00th January 20xx

DOI: 10.1039/x0xx00000x

www.rsc.org/

Vijay Kumar Das,[a] Pranjal Bharali,[b] Bolin Kumar Konwar,[b] Jyri-Pekka Mikkola,[c] Andrey Shchukarev[d] and Ashim Jyoti Thakur[a]

An endeavour has been made for the synthesis of uracil based compounds in good to high yields catalyzed by nano-Ag at 70 °C by reacting 6-Amino-1,3-dimethyluracil and indole derivatives. The catalyst was potentially recyclable from fresh up to the third run.

Apart from its multifarious involvements[1] in the field of science and technology, nanoparticles (NPs) have been sparking an explosive growth as nanocatalysis[2] being the frontiers between the homogeneous and heterogeneous catalysis.[3] Recently, the distinguished catalytic actions[4] of Ag NPs have been investigated for several organic transformations. Nano sized Ag has also been broadly used as antimicrobial agent as well as growth retardants of mold, harmful spores and germs.[5] Silver nanomaterials are seriously engaged in the manufacture of consumer commodities.[6] Still, Ag NPs have also occupied a place in imaging and immune detection.[7] The synthesis of Ag NPs by employing benign bio-surfactants as potential greener stabilizers[8] has been hot topic of research in recent years due to their unique structural diversity, high specificity, higher biodegradability, biocompatibility and digestibility, ecofriendliness, reusability, stability under extreme conditions such as high temperature, pH and salinity, low toxicity, widespread applicability and production from the renewable sources, mainly from wastes.[9] However, application of Ag NPs in organic synthesis is not explored satisfactorily. In our endeavour to exploit such aspect that too for bioactive molecules has prompted us to undertake this project. Pyrimidine analogues and its derivatives have attracted the chemists due to their interesting biological and chemotherapeutic importances.[10] In essence, the synthesis of pyrimidine derivatives can be facilitated due to it's nucleophilic C-5 position[11] and the presence of an amino group at C-6 position enhances its nucleophilicity dramatically.[12]

In our research program for the advancement of 'NOSE' (**N**anoparticles-catalyzed **O**rganic **S**ynthesis **E**nhancement)[13] chemistry, we herein report one-pot synthesis of 6-Amino-1,3-dimethyl-5-indolyl-1*H*-pyrimidine-2,4-dione derivatives from 6-amino-1,3-dimethyluracil and indole derivatives at 70 °C in DMSO catalyzed by biosurfactant capped Ag NPs (Scheme 1). Our group has long history of working on uracil compounds.[14]

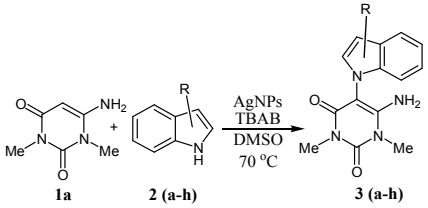

Scheme 1 Synthesis of uracil based compounds

We first prepared Ag NPs using rhamnolipid biosurfactant under mild condition[15] followed by characterisation. The thermal decomposition was studied by thermo-gravimetric analysis [Fig 1(a)] that showed two steps thermal degradation begining at 160 °C and completed above 310 °C. The first weight loss was attributed to the evaporation of physically absorbed water in air and the second weight loss may be due to the decomposition of precursor which was completed at this temperature. Figure 1(b) represents the X-ray diffraction

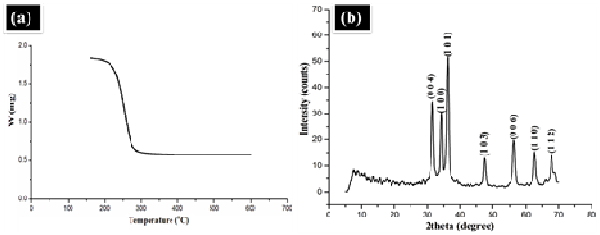

Figure 1. (a) TGA curve and (b) XRD pattern of Ag NPs

[a] *Department of Chemical Sciences, Tezpur University, Napaam, Tezpur, Assam, India, Fax: (+)91(3712)267005/6. E-mail: ashim@tezu.ernet.in.*
[b] *Department of Molecular Biology and Biotechnology, Tezpur University, Napaam-784028, Tezpur, Assam, India*
[c] *Technical Chemistry, Department of Chemistry, Umeå University, SE-90187 Umeå, Sweden*
[d] *Industrial Chemistry & Reaction Engineering, Johan Gadolin Process Chemistry Centre, Åbo Akademi University, FI-20500 Åbo-Turku, Finland*

† Electronic Supplementary Information (ESI) available: General experimental methods, SAED pattern of nano-Ag, Physical and spectroscopic data for the compounds, ^{1}H and ^{13}C NMR spectra of selected compounds. See DOI: 10.1039/x0xx00000x

pattern of Ag NPs. The sample produced peaks corresponding to (0 0 4), (1 0 0), (1 0 1), (1 0 3), (0 0 6), (1 1 0) and (1 1 2) planes. Also, Ag NPs exhibited hexagonal primitive lattice structure (JCPDS data card no 87-0598). The crystal size of Ag NPs was determined by Scherer equation considering the two highest peaks (0 0 4) and (1 0 1), and were found to lie between 11 and 16 nm respectively. Also, the planes (0 0 4), (1 0 0), (1 0 1) and (0 0 6) with their respective D spacing values have been identified in the SAED pattern (see ESI) proving that crystal structure reflection of nano-Ag.

The external morphology studied by SEM (Fig 2) presents an overview of spherical shaped Ag NPs in the network of each other. In addition, the material exhibits uniform morphology and particle size distribution.

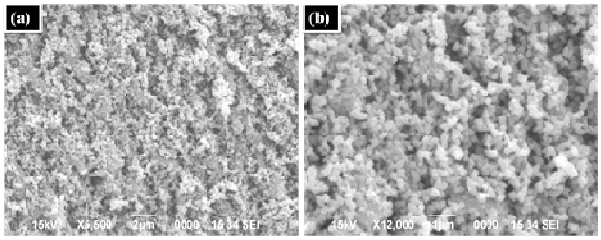

Figure 2. SEM images of Ag NPs at (a) 2 µm scale and (b) 1 µm scale

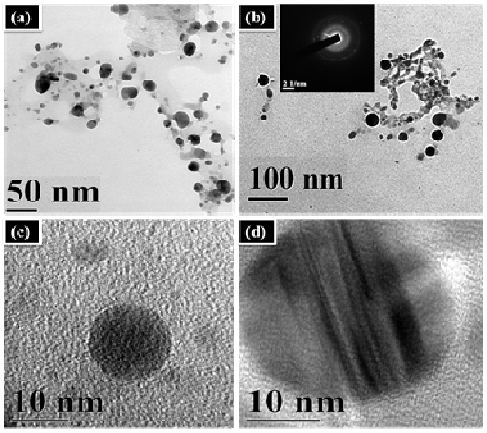

Figure 3. TEM images of nano-Ag at (a) 50 nm, (b) 100 nm, (c) 10 nm and (d) 10 nm scale

TEM investigations of nano-Ag disclosed that the particles were spherical in shape (Fig 3). The average particle size from the TEM images was calculated manually. Figure 3a revealed the bimodal presence of both smaller and larger size particles with average diameters of 1.67 nm and 11.11 nm respectively. The particles having average diameter of 22.51 nm could also be seen with some agglomerations [Fig. 3(b)]. The single particles are depicted in figures 3c and 3d respectively at 10 nm scale. The SAED pattern (embedded in Fig 3b) illustrates an overview of the crystallinity of nano-Ag.

In line with the idea of synthesizing uracil derivatives, we considered a model reaction between *N,N*-dimethyl-6-amino uracil **1** and indole **2** in the presence of K_2CO_3 base to form **3** (not previously reported) and optimized the reaction condition (Table 1). Performing the reaction as neat using **1**, **2** and K_2CO_3 by grinding in mortar and pestle, stirring in water at room

Table 1. Catalyst screening and optimization[a]

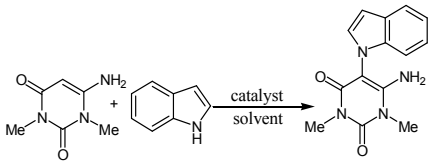

Entry	Conditions[a]	Yield (%)[b]
1	No catalyst, K_2CO_3, no solvent, room temperature, grinded, 3h	[c]
2	No catalyst, K_2CO_3, no solvent, room temperature, 19h	[c]
3	No catalyst, K_2CO_3, H_2O, room temperature/70 °C, 19h	[c]
4	No catalyst, K_2CO_3, MeOH, 70 °C, 12h	[c]
5	No catalyst, K_2CO_3, EtOH, 70 °C, 12h	[c]
6	No catalyst, K_2CO_3, DMSO, 70 °C, 16h	[d]
7	No catalyst, K_2CO_3, DMF, 70 °C, 16h	[c]
8	No catalyst, K_2CO_3, MeCN, 70 °C, 16h	[c]
9	No catalyst, K_2CO_3, Toluene, 70 °C, 16h	[c]
10	No catalyst, K_2CO_3, THF, 16h	[d]
11[e]	Nano-Ag, K_2CO_3, DMSO, 70 °C, 10h	57
12[f]	Nano-Ag, K_2CO_3, DMSO, 70 °C, 7h	47
13[g]	Nano-Ag, K_2CO_3, DMSO, 70 °C, 9h	42
14[h]	Nano-Ag, K_2CO_3, DMSO, 70 °C, 6h	68
15[h]	Nano-Ag, TBAB (5 mmol), K_2CO_3, DMSO, 70 °C, 6h	75
16[h]	Nano-Ag, TBAB (30 mol%), K_2CO_3, DMSO, 70 °C, 6h	80
17[h]	Nano-Ag, TBAB (20 mol%), K_2CO_3, DMSO, 70 °C, 6h	83
18[h]	Nano-Ag, TBAB (10 mol%), K_2CO_3, DMSO, 70 °C, 6h	85
19[h]	Nano-Ag, TBAB (7 mol%), K_2CO_3, DMSO, 70 °C, 4h	90
20[h]	Nano-Ag, TBAB (5 mol%), K_2CO_3, DMSO, 70 °C, 6h	80
21[i]	Nano-Ag, TBAB (5 mol%), K_2CO_3, DMSO, 70 °C, 8h	76
22[j]	Nano-Ag, TBAB (3 mol%), K_2CO_3, DMSO, 70 °C, 10h	58
23	No catalyst, TBAB (7 mol%), K_2CO_3, DMSO, 70 °C, 8h	[c]
24[h]	Nano-Ag, TBAB (7 mol%), Na_2CO_3, DMSO, 70 °C, 4h	88
25[h]	Nano-Ag, TBAB (7 mol%), NaOH, DMSO, 70 °C, 4h	85
26[h]	Bulk-$AgNO_3$, TBAB (7 mol%), K_2CO_3, DMSO, 70 °C, 4h	44
27[h]	Nano-MgO, TBAB (7 mol%), K_2CO_3, DMSO, 70 °C, 4h	7
28[h]	Nano-S, TBAB (7 mol%), K_2CO_3, DMSO, 70 °C, 4h	Trace
29[h]	Nano-Al_2O_3, TBAB (7 mol%), K_2CO_3, DMSO, 70 °C, 4h	5
30[h]	Nano-Ag, TBAB (7 mol%), K_2CO_3, DMSO, 120 °C, 4h	78

[a)] Reaction condition: **1** (5 mmol, 775 mg), **2** (5 mmol, 586 mg), K_2CO_3/Na_2CO_3/ NaOH (5 mmol, 690/530/200 mg), solvent (5 mL). [b)] Isolated yield. [c)] No reaction. [d)] Unknown mixture. [e)] 10 mol% catalyst. [f)] 15 mol% catalyst. [g)] 20 mol% catalyst. [h)] 7 mol% catalyst. [i)] 5 mol% catalyst. [j)] 3 mol% catalyst.

temperature/70 °C could not yield 3 (Table 1, entries 1-3). Screening of solvents (Table 1, entries 4-10) resulted in the formation of unknown mixtures in DMSO (Table 1, entry 6) and THF (Table 1, entry 10). These results indicated the requirement of a catalyst for the maximum conversion of **1** and **2** into **3**. Initially, when nano-Ag (10 mol%) was introduced, only 57% of **3** was obtained (Table 1, entry 11). Later on, an increase in catalyst loading to 15 and 20 mol% decreased the yield of **3** (Table 1, entries 12, 13). A plausible reason is due to the aggregation of Ag NPs which might have reduced the surface area by blocking the active sites. Minimising the catalyst loading to 7 mol%, better yield (Table

1, entry 14) was observed. Interestingly, when tetrabutylammonium bromide (TBAB) was used in same equivalent with respect to **1**, **2** and K_2CO_3, yield of **3** was slightly enhanced (Table 1, entry 15). When the loading of TBAB was decreased to 30 mol% the yield of **3** was again increased (Table 1, entry 16) and the best result was obtained at 7 mol% akin to Ag NPs (Table 1, entries 17-19). It is noteworthy to mention that keeping nano-Ag loading constant (7 mol%) and reducing the amount of TBAB (5 mol%) could not further improve the yield of **3** (Table 1, entry 20). Declining the loading of both nano-Ag and TBAB in an equal mol% (1:1) also could not raise the yield of **3** (Table 1, entries 21 and 22). It was also observed that TBAB alone could not catalyze the reaction (Table 1, entry 23). Thus, it was deduced that TBAB enhanced the catalytic activity of nano-Ag for the maximum conversion of **1** and **2** into **3** when 7 mol% of both of them were used but below that optimum level the yield of **3** was found lower which might be attributed to the decrease in number of active sites on the surface of the catalyst. Next, the use of Na_2CO_3 and NaOH were not preferable on the rate of the reaction and yield of **3** (Table 1, entries 24 and 25). Interestingly, when the model reaction was performed in the presence of $AgNO_3$, it could not furnish **3** in high yield as done by nano-Ag (Table 1, entry 26) confirming nano-Ag's requirement. With other nanocatalysts, trace to poor yield of 3 was observed (Table 1, entries 27-29). Performing the reaction at 120 °C bestowed **3** in lower yield (Table 1, entry 30). Overall, the reaction was observed clean using 7 mol% nano-Ag in DMSO at 70 °C and no side product formation took place.

Encouraged by these outcomes, we next generalized the reaction considering different indole derivatives and the results are summarized in table 2. It is apparent that presence of both electron donating and withdrawing groups in indole provided good yields of uracil derivatives. Indole, 2-methylindole and 3-methylindole underwent reaction with **1** to produce the desire products in good yields (table 2, entries 1-3). Indole-3-carboxylic acid, Indole-3-propanoic and indole-3-butyric acid afforded 26%, 30% and 34% yields of the products recorded under the present reaction condition which was not satisfactory, therefore, loading of both of them were increased to 10 mol% that enhanced the yields (table 2, entries 4-6). The possible cause for this outcome might be the presence of bulky groups in the substrate. Indole-3-acetonitrile also smoothly underwent reaction furnishing the product (table 2, entry 7). 5-Bromoindole bestowed the preferred product in good yield (table 2, entry 8). Indol-3-ol and Indol-4-ol afforded the desire compounds in slightly lower yields (table 2, entries 9 and 10).

The mechanism of the reaction is not clear at this moment, however, a plausible mechanism has been proposed (scheme 2). It is hypothesized that nano-Ag has activated (**I**), first, for the abstraction of proton by base and further, for the nucleophilic attack by (**IV**) to form the intermediate (**III**). It is thought that DMSO has played a dramatic role by solvating (**III**) but not (**IV**) thereby separating them. This leaves a relatively free (**IV**) which would be expected to be more reactive nucleophile.[16] Finally, deprotonation by TBAB afforded the desired product.

Table 2. Nano-Ag catalyzed synthesis of uracil derivatives

Entry	Indole derivatives	Products	Time (h)	Yield (%)[a,b]
1	Indole (**2a**)	**3a**	4	84
2	2-methyl indole (**2b**)	**3b**	7	80
3	3-methyl indole (**2c**)	**3c**	7	80
4[c]	Indole-3-carboxylic acid (**2d**)	**3d**	10	70
5[c]	Indol-3-propanoic acid (**2e**)	**3e**	10	64
6[c]	Indol-3-butanoic acid (**2f**)	**3f**	10	62
7[d]	Indol-3-acetonitrile (**2g**)	**3g**	8	78
8	5-bromo indole (**2h**)	**3h**	5	81
9	Indol-3-ol (**2i**)	**3i**	11	56
10	Indol-4-ol (**2j**)	**3j**	11	55

[a)] Isolated yield. [b)] Products were characterized by IR and NMR (^{1}H and ^{13}C) spectroscopy, MS, and also by comparing their melting points with the authentic ones. [c)] 10 mol% (nano-Ag and TBAB) was used. [d)] Brownish yellow viscous oil.

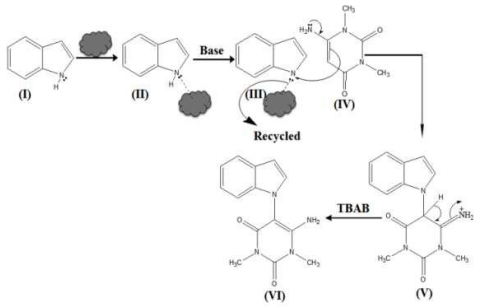

Scheme 2 Tentative reaction mechanism for the formation of **3a**

Next, we focused on the reusability of nano-Ag by considering the model reaction. As indicated in table 3, the nano-Ag was found to be active from fresh up to the 3rd run and after that its activity slightly declined. The TONs also remained constant up to the 3rd run and after that it lowered. To detect the cause for poorer yield of the product and deactivation of the catalyst, the TEM images of nano-Ag after 3rd [Fig 4(a)] and 6th [Fig 4(b)] runs were recorded. It could be observed from these figures that nano-Ag started aggregating giving larger particles which might have reduced the surface area and blocked the active sites and hence, deactivated the catalyst.

The loss in activity of the catalyst after 3rd and 4th runs was also evaluated by comparing the X-ray diffraction patterns of the aforementioned cycles. The XRD patterns [Fig 5(a)] after 3rd and 4th runs presented the unchanged morphology demonstrating the negligible loss of leaching and loss of ions from the surface of Ag NPs. This was also supported by ICP-AES data. Again, the oxidation state of the catalyst after 6th run was confirmed by XPS analysis [Fig 5(b)]. The XPS data confirm that the particles are metallic silver having 3d5/2 photoelectron line binding energy at 368 eV along with Ag M4N5N5 Auger line kinetic energy value at 357.9 eV. These data support that the catalyst did not oxidize during the recycling and retained the metallic form throughout the experiment.

Table 3. Catalyst reusability test

No. of cycles[a]	Fresh	Run 1	Run 2	Run 3	Run 4	Run 5	Run 6
Yield (%)[b]	90	90	90	90	88	84	80
Time (h)	4	4	4	4	7	10	14
TON	25.7	25.7	25.7	25.7	25.1	24.0	22.8
TOF (h-1)	6.42	6.42	6.42	6.42	3.58	2.40	1.62

[a)] Reaction conditions: **1** (10 mmol, 1550 mg), **2** (10 mmol, 1170 mg), K_2CO_3 (10 mmol, 1380 mg), DMSO (10 mL), TBAB (7 mol%, 225 mg), nano-Ag (7 mol%, 76 mg), 70 °C. [b)] Yields refer to the isolated pure products.

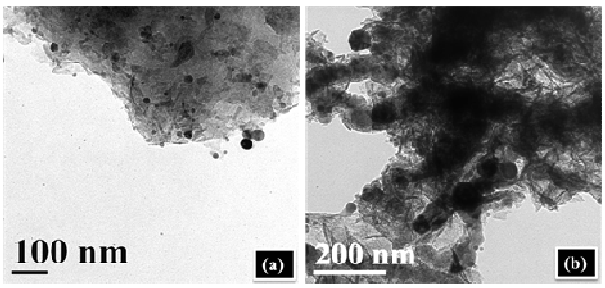

Figure 4. TEM images of nano-Ag after (a) 3rd run and (b) 6th run

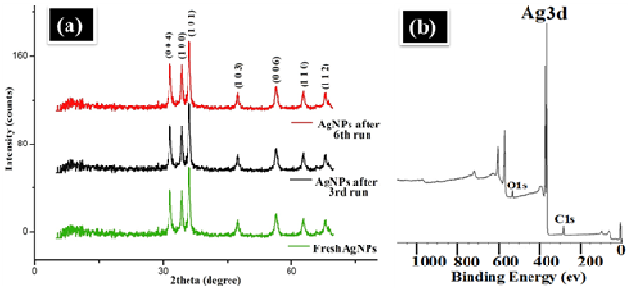

Figure 5. XRD patterns and XPS image of reused nano-Ag

We have developed an efficient protocol for the synthesis of uracil derivatives catalyzed by heterogeneous, recyclable and moisture stable nano-Ag. The reaction was optimized with respect to various parameters. We anticipate that this work would find broad applications for new chemical transformations including the synthesis of challenging bioactive compounds and complex natural products.

Experimental

Representative procedure for the synthesis of 3a. A mixture of 1,3-dimethyl-6-aminouracil 1a (0.155 g, 1 mmol), indole 2a (0.117 g, 1 mmol), TBAB (0.023 g, 7 mol%), and nano-Ag (0.0074 g, 7 mol %) were taken in a mortar where DMSO (5 mL) was added and grinded with a pestle to ensure proper mixing. The grinded mixture was transferred to a round-bottom flask (50 mL) and placed in a preheated oil bath at 70 °C under SFRC under stirring in aerobic condition for the required time (TLC). After completion (TLC), the reaction mixture was brought down to room temperature and DMSO was removed in vacuo. Then ethyl acetate (5 mL) was added to it. It was then ultracentrifuged (3,500 rpm) to pellet out the nano-Ag. The separated catalyst was washed with hot ethanol (3 × 10 mL), decanted, and finally dried in an oven at 100 °C. The reaction mixture containing the desired product was purified either by column chromatography or TLC. This procedure was followed for all the products listed in Table 2.

VKD thanks UGC for Rajiv Gandhi National Fellowship to him.

Notes and references

1 M. Horie, H. Kato, K. Fujita, S. Endoh and H. Iwahashiet, *Chem. Res. Toxicol.* 2012, **25**, 605.
2 R. Narayanan, M. A. El-Sayed, *J. Phys. Chem. B* 2004, **108**, 8572.
3 D. Astruc, F. Lu and J. R. Aranzaes, *Angew. Chem., Int. Ed.* 2005, **44**, 7852.
4 (a) Y. Mikami, A. Noujima, T. Mitsudome, T. Mizugaki, K. Jitsukawa, K. Kaneda, *Tetrahedron Lett*. 2010, **51**, 5466; (b) T. Mitsudome, Y. Mikami, H. Funai, T. Mizugaki, K. Jitsukawa and K. Kaneda, *Angew. Chem., Int. Ed.* 2008, **47**, 138; (c) T. Mitsudome, Y. Mikami, H. Mori, S. Arita, T. Mizugaki, K. Jitsukawa and K. Kaneda, *Chem. Commun.* 2009, **22**, 3258.
5 (a) X. Chen, H. J. Schluesener, *Toxicol. Lett.* 2008, **176**, 1; (b) M. Jeyaraj, G. Sathishkumar, G. Sivanandhan, D. Mubarak Ali, M. Rajesh, R. Arun, A. Ganapathi, *Colloids Surf. B: Biointerfaces*, 2013, **106**, 86.
6 (a) A. D. Russell, W. B. Hugo, *Progr. Med. Chem.* 1994, **31**, 351; (b) S. Y. Liau, D. C. Read, W. J. Pugh, J. R. Furr, A. D. Russell, *Lett. Appl. Microbiol.* 1997, **25**, 279.
7 (a) J. Kneipp, H. Kneipp, B. Wittig, K. Kneipp, *Nanomedicine: Nanotechnology, Biology, and Medicine* 2010, **6**, 214; (b) Y. Yang, S. Matsubara, L. Xiong, T. Hayakawa, M. Nogami, *J. Phys. Chem. C* 2007, **111**, 9095.
8 (a) P. Bharali, S. Das, B. K. Konwar, A. J. Thakur, *Int. Biodeter. Biodeg.* 2011, **65**, 682; (b) M. Benincasa, A. Abalos, I. Oliveira, A. Manresa, *Antonie Van Leeuwenhoek* 2004, **85**, 1.
9 (a) G. S. Kiran, A. Sabu, J. Selvin, *J. Biotech.,* 2010, **148**, 221; (b) Kasture, M. B. P. Patel, A. A. Prabhune, C. V. Ramana, *J. Chem. Sci.* 2008, **120**, 515.
10 (a) S. Manta, E. Tsoukala, N. Tzioumaki, C. Kiritsis, J. Balzarini, D. Komiotiset, *Bioorg. Chem.* 2010, **38**, 48; (b) A. Plant, P. Thompson, D. M. Williams, *J. Org.* Chem. 2009, **74**, 4870.
11 M. Dabiri, S. C. Azimi, H. R. Khavasi, A. Bazgir, *Tetrahedron* 2008, **64**, 7307.
12 B. L. Lam, L. N. Pridgen, *J. Org. Chem.* 1986, **51**, 2592.
13 (a) V. K. Das, R. R. Devi, P. Raul, A. J. Thakur, *Green Chem.* 2012, **14**, 847; (b) V. K. Das, R. R. Devi, and A. J. Thakur, *Appl. Catal. A: Gen.* 2013, **456**, 118; (c) V. K. Das, M. Bora, A. J. Thakur, *J. Org. Chem.* 2013, **78**, 3361; (d) V. K. Das, A. J. Thakur, *Tetrahedron Lett.* 2013, **54**, 4164.
14 (a) S. Das, A. J. Thakur, T. Medhi, B. Das, *RSC Advances* 2013, **3**, 3407; (b) S. Das, A. J. Thakur, *Eur. J. Org. Chem.* 2011, **12**, 2301.
15 J. P. Saikia, P. Bharali, B. K. Konwar, *Colloids and Surfaces B: Biointerfaces* 2013, **104**, 330.
16 (a) H. E. Zuagg, D. A. Dunnigan, R. J. Michaels, L. R. Swett, T. S. Wang, A. H. Sommers, R. W. Denet, *J. Org. Chem.* 1961, **26**, 644; (b) A. J. Parker, *Quart. Rev. Chem. Soc. Lond.* 1962, **16**, 163; (c) M. Goto, K. Akimoto, K. Aoki, M. Shindo, K. Kogaet, *Tetrahedron Lett.* 1999, **40**, 8129.

A convenient 'NOSE' approach for the synthesis of 6-Amino-1,3-dimethyl-5-indolyl-1*H*-pyrimidine-2,4-dione derivatives catalyzed by nano-Ag

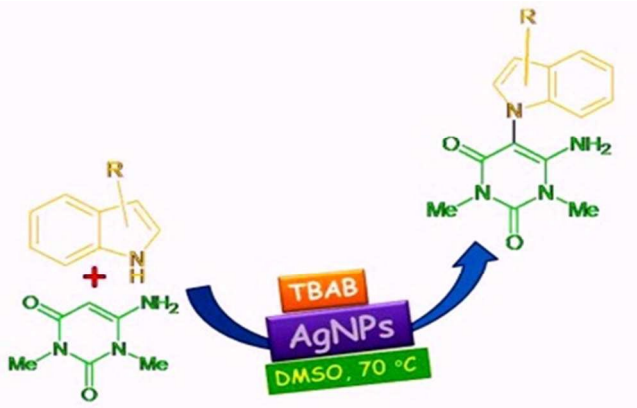

Uracil derivatives are synthesized in high yields catalyzed by reusable nano-Ag at 70 °C by reacting 6-amino-1,3-dimethyluracil and indole derivatives.